Theor Appl Genet (2014) 127:1703–1718
DOI 10.1007/s00122-014-2333-8

ORIGINAL PAPER

Transcriptome profiling of wheat differentially expressed genes exposed to different chemotypes of *Fusarium graminearum*

Khaled Al-Taweel · W. G. Dilantha Fernando · Anita L. Brûlé-Babel

Received: 10 October 2013 / Accepted: 15 May 2014 / Published online: 4 June 2014
© Springer-Verlag Berlin Heidelberg 2014

Abstract

Key message **The study is an overview of the behavior of the wheat transcriptome to the *Fusarium graminearum* fungus using two different chemotypes. The transcriptome profiles of seven putative differentially expressed defense-related genes were identified by SSH and further examined using qPCR.**

Abstract Fusarium head blight (FHB) of wheat (*Triticum aestivum* L.), caused by several species of the fungus fusarium, is important in all wheat growing regions worldwide. The most dominant species in Canada is *Fusarium graminearum* (Fg). *F. graminearum* isolates producing mycotoxins such as 3-acetyl-deoxynivalenol (3ADON) and 15-acetyl-deoxynivalenol (15ADON). The objective of this study was to investigate the effect of the different chemotypes of Fg on the transcriptome pattern of expressed wheat genes. A cDNA library was constructed from infected "Sumai 3" spikes harvested at different times after inoculation with a macroconidia suspension. Employing suppression subtractive hybridization (SSH), the subtracted cDNA library was differentially screened by dot-blot hybridization. Thirty-one clones were identified; one was isolated and characterized, and transcriptome profiling of seven up-regulated putative defense-related genes was performed using quantitative real-time reverse-transcriptase PCR. These genes may be involved in the wheat-pathogen interactions revealing transcript accumulation differences between the non-diseased, 3ADON-, and 15ADON-infected plants. Additionally, significant differences in gene expression were observed between 3ADON- and 15ADON-infected plants which highlight the significance of a particular chemotype in FHB disease.

Abbreviations

15ADON	15-Acetyl-deoxynivalenol
3ADON	3-Acetyl-deoxynivalenol
DON	Deoxynivalenol
Fg	*Fusarium graminearum*
FHB	Fusarium head blight
NIV	Nivalenol
SSH	Suppression subtractive hybridization
UGT	UDP-glucosyltransferase

Introduction

Fusarium head blight (FHB), caused by *Fusarium graminearum* (Fg), is a destructive disease of wheat and barley worldwide. Considerable losses both in quantity and grain quality are known to take place when grain is contaminated with harmful trichothecenes, among which deoxynivalenol (DON) is one of the most important (Windels 2000). Mycotoxin contamination in grain can seriously affect animal

Communicated by Xianchun Xia.

Electronic supplementary material The online version of this article (doi:10.1007/s00122-014-2333-8) contains supplementary material, which is available to authorized users.

K. Al-Taweel · W. G. D. Fernando (✉) · A. L. Brûlé-Babel
Department of Plant Science, University of Manitoba, Winnipeg, MB R3T 2N2, Canada
e-mail: dilantha.fernando@umanitoba.ca

A. L. Brûlé-Babel
e-mail: anita.brulebabel@ad.umanitoba.ca

K. Al-Taweel
Department of Biotechnology, General Commission of Agricultural Scientific Research (GCASR), P.O. Box 113 Douma-Damascus, Syria
e-mail: khaledta72@gmail.com

and human health. As a result, rigid standards have been set for tolerable levels of DON in wheat flour (Placinta et al. 1999; Sugita-Konishi and Kumagai 2005). It is most likely that DON plays an important role in pathogenicity as a virulence factor that triggers defense response genes during infection. Wheat tissue treated with DON shows typical FHB symptoms, and the pathogenicity of *F. graminearum* depends on its DON producing ability (Xie and Wang 1999). In wheat, resistance to DON is classified as Type III resistance and is reflected by its ability to prevent the synthesis of DON or in the detoxification of DON (Miller and Arnison 1986; Yu et al. 2008).

Breeding wheat resistant to FHB is one of the best choices to minimize crop and grain quality losses caused by the disease. Consequently, the absence of visible host responses or disease symptoms in the early stages following pathogen inoculation has stimulated investigations of the underlying nature of the host-pathogen interaction between wheat and *F. graminearum*. FHB infection is initiated in wheat florets at anthesis by pathogen ascospores and on occasion by macroconidia. After FHB infection, florets become necrotic or bleached in appearance and may have a pinkish or orangish appearance near their base. Infected grains do not fill properly resulting in low test weight and shriveled seeds. It is proposed that DON produced by FHB inhibits protein production and may play a role in the infection process (Kang and Buchenauer 1999; Ansari et al. 2014). Cytological studies show a reduction in cell wall components, elucidating the importance of cell wall degrading enzymes during infection of wheat spikes by *Fusarium culmorum* (Kang and Buchenauer 2000a). As the infection progresses, florets of infected spikes become increasingly necrotic and bleached, leading to a reduction in grain yield and quality.

Wheat responds to *F. graminearum* infection by inducing various defense reactions. In resistant wheat cultivars, during infection by *F. graminearum*, the thickness of cell wall increases rapidly due to deposition of lignin content compared to uninoculated plants (Kang and Buchenauer 2000b). In contrast, only a slight increase in lignin was detected in inoculated susceptible cultivars compared to uninoculated plants (Kang and Buchenauer 2000b), suggesting that lignin restrains fungal infection. Multiple studies showed that the transcription levels for different categories of biotic and abiotic stress-related genes were increased upon *F. graminearum* inoculation in both partially resistant and susceptible cultivars (Pritsch et al. 2000; Kruger et al. 2002). The expression of biotic and abiotic stress-related genes may result in a reduction of FHB severity in wheat, but the relationship and mode of interaction between FHB resistance and *F. graminearum* have not been clearly established. Hallen-Adams et al. (2011) reported a negative correlation between the amount of DON and expression of trichothecene biosynthesis genes in susceptible wheat cultivar, Wheaton. Another study done by Schmidt-Heydt et al. (2010) presented a polynomial model that shows the relationship between actual/predicted DON production relative to the expression of the *tri* genes and environmental factors. Identifying host genes differentially expressed in response to the pathogen may help illustrate cellular processes activated or repressed during the early phase of host–pathogen interactions. These interactions may ultimately determine the extent of fungal colonization.

FHB resistance is a quantitative trait, which is usually controlled by a few major genes and several other minor genes (Buerstmayr et al. 1997, 1999). Mapping of quantitative trait loci (QTL) has been widely used to determine the effect of QTL underlining quantitative traits. To date, FHB-associated QTL have been reported from about 50 wheat cultivars covering all 21 chromosomes (Liu et al. 2009). Among them QTL on 3BS, formally designated as *Fhb1*, shows the largest effect on spread of infection within the spike (type II resistance) and accumulation of DON (type III resistance). Sumai 3, the cultivar tested in this study, and its derivatives carry *Fhb1* and are the most frequently used source of FHB resistance in breeding programs worldwide (Buerstmayr et al. 2009). The QTL on chromosomes 5A, 6B, 3A, 4B, 2D, 1B, 7A, 5B, and 3B also have been mapped in more than two populations in the previous studies and are considered to be stable QTL (Cuthbert et al. 2006; Liu et al. 2009). Several wheat varieties have been identified as sources of FHB resistance, among which Sumai 3 is one of the most important genetic resources for FHB resistance research and breeding. However, Sumai 3 has poor agronomic traits. Genetic linkage drag of undesirable traits is frequently observed when Sumai 3 is used as resistant gene donor in traditional breeding strategies. Insertion of cloned resistance genes into susceptible varieties with good agronomic traits using genetic engineering and molecular biological techniques could circumvent the problems associated with linkage drag. Several genes related to DON resistance have been cloned from various crop species, such as acetyltransferase in wheat (Mitterbauer and Adam 2002) and the ribosomal protein L3 (RPL3) gene in rice (Harris and Gleddie 2001) and wheat (Lucyshyn et al. 2007).

Trichothecene chemotype variation has received considerable attention in analyses of Fusarium populations that cause FHB (Xu and Nicholson 2009). In North America, there are two *F. graminearum* chemotypes traditionally responsible for FHB, known as the 15-acetyl-deoxynivalenol (15ADON) and 3-acetyl-deoxynivalenol (3ADON) chemotypes. Surveys indicate the displacement of the existing 15ADON population by the 3ADON population

in some regions of North America (Ward et al. 2008; Guo et al., 2008). Moreover, the 3ADON population is more aggressive and produces a higher level of DON than the 15ADON population in wheat (Goswami and Kistler 2004; Ward et al. 2008; Puri and Zhong 2010). Population genetic analyses using DNA markers revealed a significant genetic differentiation between the two populations (Puri and Zhong 2010). Surveys of *F. graminearum* from China and Japan identified strains with the 3ADON, 15ADON, and Nivalenol (NIV) chemotypes, and in China, DON strains are displacing NIV strains (Zhang et al. 2010). There is also evidence for shifts in trichothecene chemotypes of *F. graminearum* in Europe (Waalwijk et al. 2003).

The genetic basis for production of 3ADON versus 15ADON has not yet been fully determined. The trichothecenes produced by *F. graminearum* differ by the presence and absence of acetyl functions at C3 and C15; 3ADON has a C3 acetyl group, whereas 15ADON has a C15 acetyl group. Alexander et al. (2011) proved that the *Tri8* gene is the primary determinant of the 3ADON and 15ADON chemotypes in Fusarium, indicating that *Tri8* from 3ADON strains catalyzes C15 deacetylation of 3,15-diADON to yield 3ADON, whereas *Tri8* from the 15ADON strain catalyzes C3 deacetylation of 3,15-diADON to yield 15ADON. Although molecular mapping of quantitative trait loci for FHB resistance has been extensively reported, studies on the genetic and genomic basis for the 3ADON versus 15ADON chemotypes and their impact on host wheat genes have not been elucidated (Alexander et al. 2011). To date, little research has been done on genes involved in the interaction between *F. graminearum* and wheat. In spite of the apparent shifts in trichothecene chemotypes among *F. graminearum* that causes FHB, the transcriptome profiling of wheat genes that respond to the different chemotypes has not yet been studied.

One goal in the present study was to identify wheat genes that are differentially expressed during the resistance response to the 3ADON chemotypeof *F. graminearum* using suppression subtractive hybridization (SSH). The second goal was to obtain a more thorough understanding of the behavior of host genes under infection by different chemotypes (3ADON/15ADON) of *F. gaminearium*. This information could help in further understanding resistance mechanisms of wheat in response to Fusarium infection. Additionally, this study investigates the difference in gene expression in wheat infected by two different FHB-chemotypes compared to the control, and hence may aid the development of an effective strategy for control of wheat FHB. To our knowledge, this is the first study on global expression profiling of FHB-related genes of wheat infected by two different Fusarium chemotypes conducted using SSH to reveal differentially expressed genes under FHB infection.

Materials and methods

Plant material

Wheat (*Triticum aestivum* L.) line "Sumai 3", selected from the cross Funo/Taiwan wheat and exhibiting resistance to FHB, was used in this study. Plants were grown in a controlled environment growth cabinet with a 16-h photoperiod and 18/15 °C day/night temperatures. Plant-Prod (20-20-20) all-purpose fertilizer (Brampton, ON, Canada) was applied at a rate of 6 g/L every second week.

Pathogen and inoculation

Two *F. graminearum* isolates were used. Fg2 produces 3ADON, and Fg35 produces 15ADON. Inoculum concentration was 1×10^5 conidia/mL (Al-Taweel et al. 2011). Two florets above the ten basal spikelets were inoculated with 10 μL of a conidia suspension each, while control samples were inoculated with water. The spikes were covered with transparent plastic bags for 72 h to standardize humidity content after inoculation. The infected spikes were harvested 6, 12, 24, 36, 48, 72, and 144 h after inoculation (hai), immediately immersed in liquid nitrogen, and then stored at −80 °C until processed. Later, the total RNA was isolated from FHB- and water-inoculated spikes for the construction of a subtracted cDNA library, which is summarized in Online Resource 1.

RNA isolation, mRNA purification, and cDNA library construction

Total RNA was isolated, and mRNA was purified from the 3ADON-, 15ADON-, and water-inoculated spikes (control). A cDNA library was constructed using pooled mRNA isolated from Fg2-infected spikes harvested at 6, 12, 24, 36, 48, 72, and 144 hai as described by Al-Taweel et al. (2011).

Suppression subtractive hybridization (SSH)

cDNA synthesis and subtraction from the pooled poly(A) + RNA were performed using a PCR-Select™ cDNA Subtraction Kit (Clontech, Palo Alto, CA, USA) according to the manufacturer's instructions (Online Resource 2). The cDNA that contained transcripts from 3ADON-inoculated spikes of Sumai 3 was referred to as the "tester", whereas the cDNA from the water-inoculated spikes of Sumai 3 was referred to as the "driver". The tester and driver cDNAs were digested with *Rsa*I, yielding short blunt-ended molecules. The tester cDNA was then divided into two groups: forward subtraction (the tester subtracted against the driver) and reverse subtraction (the driver subtracted against the tester). Each group was ligated with

different cDNA adaptors. Two hybridizations were then performed for the subtraction of sequences common to both cDNA populations using an excess of driver cDNA, and the overhang ends were filled in with DNA polymerase to make different annealing sites for the nested primers on their 3′ ends. The entire cDNA population was then subjected to PCR amplification using an Advantage2 PCR kit (Clontech). This PCR step allowed for normalization of the remaining fragments by suppression of undesirable PCR amplifications and exponentially enriching the differentially expressed sequences as described in the manufacturer's instructions.

Cloning and differential screening

The subtracted cDNAs (secondary PCR products) were T-A cloned into pGEM-T Easy Vector using pGEM-T Easy Vector System Kit (Promega, USA). The ligation products were transformed into *E. coli* (ElectroMAX DH10B Cells, Invitrogen) by electroporation according to the manufacturer's instructions in order to construct the subtracted cDNA library.

Prior to differential screening, about 1,000 randomly selected white-SSH clones were inoculated individually into 96-deep well plates with 500 µL of 1 × amp-LB freezing buffer and incubated with shaking at 37 °C overnight. For PCR amplification of the cDNA inserts, 1 µL of overnight culture was used along with 19 µL of master mix (Advantage2 PCR kit, Clontech) including the nested PCR primers 1 and 2R (PCR-Select cDNA Subtraction Kit). PCR was performed with the following parameters: 94 °C for denaturation and 68 °C for both annealing and extension steps according to the PCR-Select Differential Screening Kit (Clontech). After confirmation of amplification on 2 % agarose gel, equal volumes of PCR products were mixed with 0.6 N NaOH for denaturation. Subsequently, 2 µL of denatured PCR product was arrayed onto duplicate positively charged nylon membranes (Roche, Mannheim, Germany). After neutralization with 0.5 mol/L Tris–HCl, pH 7.5, and rinsing in water, the denatured cDNA inserts were UV cross linked to the membranes. The identical membranes were prehybridized for 3 h and hybridized for 16 h at 50 °C in High SDS Hybridization Buffers (Roche) containing similar amounts of Digoxigenin-labeled probes of the SSH tester and SSH driver, which were synthesized using the PCR DIG Probe Synthesis Kit (Roche) according to the manufacturer's instructions. After the washing and blocking steps, the signals were detected with anti-digoxigenin-AP (1:10,000) Fab fragments (Roche) using NBT/BCIP according to DIG Nucleic Acid Detection Kit (Roche). Then, the most promising clones that hybridized with the probe of the SSH tester but not the driver that gave significant signals were selected. These positive clones were considered to be expressed differentially in wheat infected by Fg2 (3ADON isolate).

EST sequencing and BLAST homology search

Positive clones selected by dot-blot hybridization (about 200 clones) were sequenced using universal primers T7/SP6. After exclusion of the universal and nested primers, each sequence of the isolated clones was used for homology searches applying the BLAST program (BLASTN and BLASTX) in two databases (GenBank non-redundant (nr) and EST databases) of the National Center of Biotechnology Information (NCBI; http://www.ncbi.nlm.nih.gov).

Isolation of the full-length cDNA of TaUGT5

The full-length of clone "Ta-Fg2-P0-80" that coded for TaUGT5 was obtained by screening a cDNA library of FHB-induced wheat spikes constructed by Al-Taweel et al. (2011). The gene-specific primers TaUGT5 -F (5′-ATGGCTTCTTCTATCACTAGCAGCGG-3′) and TaUGT5-R (5′-CTAGTTCCGCCCCTCCTTTGCT-3′) that flank the ORF of the gene of interest were designed. The PCR was conducted as follows: 95 °C for 2 min, followed by 35 cycles of 94 °C for 30 s, 66 °C for 30 s, and 72 °C for 1.3 min. The PCR product was excised from an agarose gel, purified (QIAquick PCR Purification Kit, Qiagen), T/A cloned into pGEM-T Easy vector, and transformed by heat shock into JM109 high efficiency competent cells using the pGEM-T Easy Vector System Kit (Promega, USA) according to the manufacturer's instructions. Once the clone with the expected amplicon length was identified, the recombinant vector was sent for sequencing in two directions using T7 and SP6 universal primers. Based on the qualified sequence, the TaUGT5 amino acid sequence was used to search for similar peptide sequences in public databases (http://www.ncbi.nlm.nih.gov) using ClustalW2 program for multiple sequence alignment. A flow chart of SSH library synthesis and characterization of the subtracted genes are shown in Online Resource 3.

Real-time quantitative reverse-transcriptase PCR (Q-RT-PCR)

Total RNA of 3ADON-, 15ADON-, and water-inoculated samples was treated with DNase I (RNeasy Plant Mini Kit, Qiagen) to remove DNA contamination before cDNA synthesis. The cDNA was synthesized from 2 µg total RNA applying oligo $(dT)_{18}$ and random hexamers using the Maxima First Strand cDNA Synthesis Kit for RT-qPCR (Fermentas) according to the manufacturer's instruction. Real-time PCR was performed on MxPro- Mx3005P QPCR

Systems (Stratagene, USA). The forward and reverse primers for Q-RT-PCR were designed from the differentially expressed clones using Primer Express version 3.0 software (Perkin-Elmer Applied Biosystems, Foster City, CA, USA), then the primers were checked for gene specificity using Primer BLAST tool at NCBI. A set of wheat Ubiquitin (UBQ) primers were also designed for use as an endogenous control to normalize the data for differences in input RNA and efficiency of reverse transcription between the various samples. After examining the efficiency of the designed and the calibrator primers, the qPCR was performed in a final volume of 20 µL containing Maxima SYBR Green/ROX qPCR Master Mix (2×) (Fermentas), 100 nM each of forward and reverse primers, and 30 ng of cDNA template. After an initial activation step of the DNA polymerase at 95 °C for 10 min, samples were subjected to 40 cycles of amplification (denature at 95 °C for 30 s, annealing and extension together at 60 °C for 1 min). Immediately after the final PCR cycle, a melting curve analysis was done to determine specificity of the reaction by incubating the reaction at 95 °C for 1 min, annealing at 55 °C for 30 s, and then slowly increasing the temperature to 95 °C for 30 s.

Quantification of target gene expression was done with the comparative C_T method (Schmittgen and Livak 2008). The C_T used in the real-time PCR quantification is defined as the PCR cycle number that crosses an arbitrarily chosen signal threshold in the log phase of the amplification curve. The relative expression level of the gene of interest was computed with respect to UBQ to account for any variance in the amount of input cDNA. Average C_T values from triplicate PCRs were normalized to average C_T values for UBQ from the same cDNA preparations. The controls, water-inoculated samples at different time points, were chosen as the calibrators, and all infected samples were quantified relative to the controls at the same time points. Statistical Analysis System (SAS) was used in all the analyses, and values of mean ± SE (Standard Error) of three independent experiments and significance of the difference between the tested samples are indicated by $*P \leq 0.05$.

Results

Evaluation of subtraction efficiency

A subtracted library was constructed to clone and identify genes showing differential expression between FHB-inoculated and water-inoculated wheat spikes. As well, the key to obtaining successful SSH results was to effectively eliminate uniform cDNA appearing in both testers and drivers. In order to evaluate the success of the subtraction, two approaches were investigated; firstly, analyzing the secondary PCR products side-by-side for subtracted- and unsubtracted-control samples (which were running along with the experimental tested samples to check the success of the procedure applied) and comparing with the marker which is ΦX174 DNA/*Hae* III digest. Figure 1 demonstrates that the major bands of the subtracted control sample correspond to the marker bands, indicating that the cDNA homologous to both tester and driver were eliminated. Secondly, the subtraction efficiency was analyzed showing the effectively reduced abundance of non-differentially expressed genes. The expression of UBQ gene, which is a constitutively expressed gene and used in this study as a housekeeping gene, was compared between subtracted and unsubtracted cDNA by RT-PCR. In subtracted cDNA, PCR products were first detected at 30 cycles, but in contrast, the amplification products of unsubtracted cDNA were first observed at 15 cycles (Fig. 2).

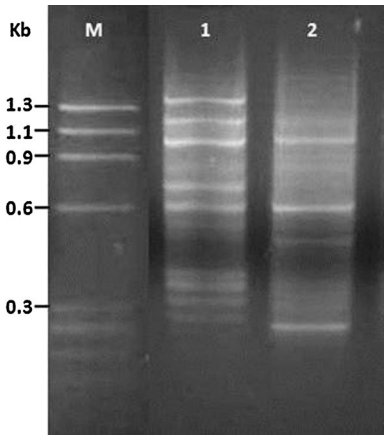

Fig. 1 Secondary PCR analysis of subtraction efficiency. The secondary PCR product of the subtracted skeletal muscle sample contains DNA fragments corresponding to the ΦX174/Hae III digest (control). The adapter sequences on both ends of DNA fragments cause the mobility shift of these PCR products in comparison with original, digested ΦX174 DNA. *Lane M* ΦX174 DNA/Hae III digest size markers. *Lane 1* Secondary PCR products of subtracted control. *Lane 2* Secondary PCR products of unsubtracted control

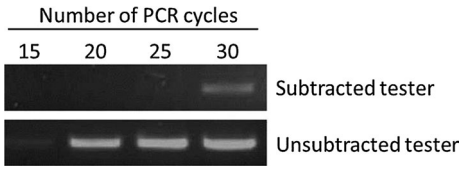

Fig. 2 Estimation of subtraction efficiency by RT-PCR. Assessment of subtractive efficiency was conducted by 15–30 cycles PCR with primers for UBQ gene in subtracted (*upper panel*) and unsubtracted (*lower panel*) tester of secondary PCR products. The numbers of PCR cycles are indicated above the panel

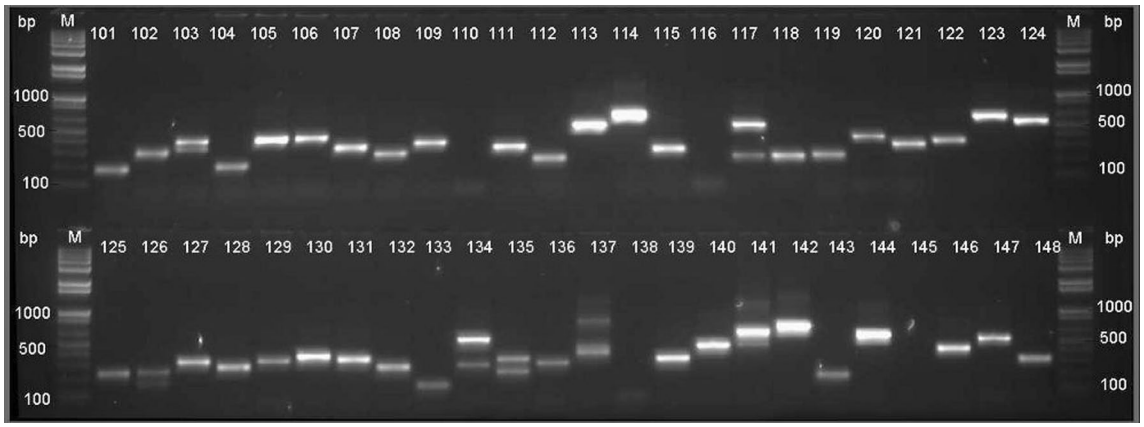

Fig. 3 PCR amplification of subtracted cDNA inserts. *Lane M* 1 kb Plus marker; *Lanes 101–148* a part of clones selected randomly and insert-amplified by clone-PCR

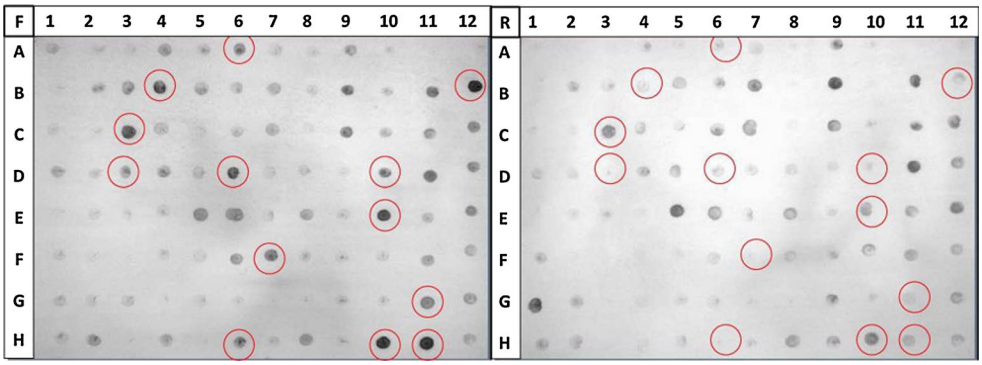

Fig. 4 Differential screening of the positive clones of the subtracted cDNA library. The two membranes are identically arrayed with PCR products of clones from the forward SSH cDNA library. *Panel F* the blotted membrane was hybridized to the probe made from the forward-subtracted SSH cDNA. *Panel R* the blotted membrane was hybridized to the probe made from the reverse-subtracted SSH cDNA. The *circled clones* show differential hybridization signals

Identification of positive clones and differential screening

The second PCR products of SSH were cloned into pGEM-T Easy vectors and preserved in *E. coli*. A total of 1000 white-clones were picked randomly from the subtracted cDNA library. Over 95 % was transformants. The inserted cDNAs were amplified by clone-PCR with nested primer 1 and 2R and were approximately 200–700 bp in length (Fig. 3). The PCR products were then arrayed on duplicate membranes for a dot-blot hybridization assay (data are shown in Online Resource 4, 5). A total of 200 positive cDNA clones (20 %) that specifically hybridized with the probe from a SSH tester, but not the driver, were screened. These candidate clones that displayed differential and significant signals were considered to be expressed differentially in wheat infected by *F. graminearum*. All positive clones were sequenced and characterized. Figure 4 shows an example of differential screening results with one duplicated pair of membranes.

Genes identified by SSH

After excluding non-relevant, noise and short sequences from the 200 sequenced clones, 126 expressed sequence tags (ESTs) were screened for non-redundant sequences and to predict putative gene functions. Seventy-five of these sequences showed significant matches to plant genes, plus 51 with significant matches to fungus *Gibberella zeae*, also known by *F. graminearum* (data are shown in Online Resource 6). Among the 75 ESTs of plant sequences, 31 clones were related to the wheat cultivar used (Table 1). After first pass sequences, these clones have been deposited as ESTs at NCBI under the names used in this study (Table 2). Out of 31 ESTs, 7 genes were selected based on their putative involvement in pathogen-defense response and/or high signal expression in differential screening. The seven clones reported in this study are Ta-Fg2-P0-80 that displayed significant similarity (99 %) to UDP-glucosyltransferase gene, Ta-Fg2-P2-H07 that showed the highest similarity (100 %)

Table 1 Homology searches of differentially expressed clones obtained by SSH for FHB-infected wheat

No.	Clone ID	Size/bp	Database	Accession No.	Species	Description	E value
1	Ta-Fg2-P0-80	723	Gene Bank nr	GU248274	*Triticumaestivum*	UDP-glucosyltransferase	0
			Gene Bank EST	CJ942671	*Triticumaestivum*	cDNA clone whchan5b02	0
2	Ta-Fg2-P0-13	215	Gene Bank nr	DQ019639	*Triticumaestivum*	Splicing regulator (SRp30a)	2.00E−102
			Gene Bank EST	CJ896445	*Triticumaestivum*	cDNA clone whthls9n17	0
3	Ta-Fg2-331	378	Gene Bank nr	EU660484	*Triticumaestivum*	GTPase SAR1 (Sar1.3)	4.00E−134
			Gene Bank EST	CJ499671	*Triticumaestivum*	cDNA clone whfl34i05	0
4	Ta-Fg2-P1-G06	285	Gene Bank nr	NM_001153075	*Zea mays*	Cytokinin-N-glucosyltransferase 1	1.00E−06
			Gene Bank EST	CJ915331	*Triticumaestivum*	cDNA clone whthkles31o06	7.00E−143
5	Ta-Fg2-P1-H12	409	Gene Bank nr	FJ459810	*Triticumaestivum*	Blue copper protein	5.00E−20
			Gene Bank EST	EB512672	*Triticumaestivum*	*Fusarium_graminearum*_inculated_wheat_heads. cDNA clone Ta08_04d16	1.00E−117
6	Ta-Fg2-P1-A11	393	Gene Bank nr	BK005645	*Triticumaestivum*	Histidine-containing phosphotransfer protein 3 (HP)	3.00E−123
			Gene Bank EST	CJ842109	*Triticumaestivum*	cDNA clone whatlal28n21	3.00E−123
7	Ta-Fg2-P1-H04	280	Gene Bank nr	AY123419	*Triticumaestivum*	Putative ribosomal protein L35	7.00E−136
			Gene Bank EST	EB515741	*Triticumaestivum*	*Fusarium_graminearum*_inculated_wheat_heads. cDNA clone Ta10c_03K08_R	1.00E−138
8	Ta-Fg2-P1-H06	241	Gene Bank nr	X58394	*Triticumaestivum*	Thaumatin-like protein	2.00E−46
			Gene Bank EST	CD863039	*Triticumaestivum*	cDNA clone AZO1105H16	5.00E−49
9	Ta-Fg2-P1-G08	171	Gene Bank nr	AJ005840	*Triticumaestivum*	Thioredoxin M	3.00E−43
			Gene Bank EST	CJ707748	*Triticumaestivum*	cDNA clone whv3n11o15	3.00E−56
10	Ta-Fg2-P1-C11	224	Gene Bank nr	AK252471	*Hordeumvulgare*	cDNA clone FLbaf161o03	2.00E−78
			Gene Bank EST	GR303360	*Triticumaestivum*	Similar to photosystem I hydrophobic protein	3.00E−108
11	Ta-Fg2-P1-G05	243	Gene Bank nr	AK336255	*Triticumaestivum*	cDNA clone SET3_J19	3.00E−120
			Gene Bank EST	CN010997	*Triticumaestivum*	Wheat *Fusarium graminearum* infected spikeCdna. cDNA clone WHE3878_F09_L18	1.00E−107
12	Ta-Fg2-P2-B01	333	Gene Bank nr	AB162961	*Hordeumvulgare*	Tryptophan decarboxylase	0
			Gene Bank EST	CJ948191	*Triticumaestivum*	cDNA clone whchul22p07	3.00E−141
13	Ta-Fg2-P2-C04	327	Gene Bank nr	AY226581	*Triticumaestivum*	Caffeic acid O-methyltransferase (COMT1) mRNA	1.00E−70
			Gene Bank EST	EB515061	*Triticumaestivum*	*Fusarium_graminearum*_inculated_wheat_heads, cDNA clone Ta10b_02m09	1.00E−165
14	Ta-Fg2-P2-C10	496	Gene Bank nr	NM_001155256	*Zea mays*	Zea mays protein phosphatase	5.00E−147
			Gene Bank EST	CJ900699	*Triticumaestivum*	cDNA clone whthkles22p20	0
15	Ta-Fg2-P2-C11	328	Gene Bank nr	EU595568	*Triticumaestivum*	Peroxidase class III	1.00E−92
			Gene Bank EST	CJ963527	*Triticumaestivum*	cDNA clone whchul32i24	3.00E−94
16	Ta-Fg2-P2-E10	448	Gene Bank nr	M76685	*Zea mays*	Zea mays tryptophan synthase beta-subunit (TSB2) mRNA	1.00E−141
			Gene Bank EST	EB512356	*Triticumaestivum*	*Fusarium_graminearum*_inculated_wheat_heads, cDNA clone Ta08_02i18	0
17	Ta-Fg2-P2-F04	239	Gene Bank nr	AB029936	*Triticumaestivum*	Chitinase 3	2.00E−85
			Gene Bank EST	CJ913579	*Triticumaestivum*	cDNA clone whthkles26l13	2.00E−85

Table 1 continued

No.	Clone ID	Size/bp	Database	Accession No.	Species	Description	E value
18	Ta-Fg2-P2-H07	165	Gene Bank nr	AJ890250	*Triticumaestivum*	Putative glucan endo-1,3-beta-D-glucosidase.	2.00E−75
			Gene Bank EST	CV770019	*Triticumaestivum*	Library 2 Gate 3 Triticumaestivum cDNA	3.00E−75
19	Ta-Fg2-P2-H12	680	Gene Bank nr	DQ355953	*Oryza sativa*	Receptor kinase (TRKd)	9.00E−121
			Gene Bank EST	CJ628390	*Triticumaestivum*	cDNA clone whcs15e17	0
20	Ta-Fg2-P2-F08	486	Gene Bank nr	AB055077	*Triticumaestivum*	Tamdr1 mRNA for multidrug resistance protein	0
			Gene Bank EST	EB511886	*Triticumaestivum*	*Fusarium_graminearum*_inculated_wheat_heads, cDNA clone Ta07b_02e11	0
21	Ta-Fg2-P2-G10	289	Gene Bank nr	DQ435667	*Triticumaestivum*	Alpha tubulin-4B (TUBA-4B) mRNA	5.00E−125
			Gene Bank EST	CN012746	*Triticumaestivum*	Wheat *Fusarium graminearum* infected spike cDNA library Triticumaestivum cDNA clone WHE3952_ D08_G16	8.00E−142
22	Ta-Fg2-P2-G11	315	Gene Bank nr	X66428	*Hordeumvulgare*	Photosystem I subunit N	1.00E−32
			Gene Bank EST	EV253782	*Triticumaestivum*	Similar to photosystem I subunit N	7.00E−42
23	Ta-Fg2-P2-B06	243	Gene Bank nr	AK336255	*Triticumaestivum*	cDNA clone SET3_J19	7.00E−104
			Gene Bank EST	CN009260	*Triticumaestivum*	Wheat *Fusarium graminearum* infected spike cDNAlibrary, cDNA clone WHE3856_F08_K16	2.00E−117
24	Ta-Fg2-P2-D11	192	Gene Bank nr	AK336255	*Triticumaestivum*	cDNA clone SET3_J19	1.00E−92
			Gene Bank EST	AL822074	*Triticumaestivum*	cDNA clone D07_N130	4.00E−80
25	Ta-Fg2-P2-E08	430	Gene Bank nr	AK331790	*Triticumaestivum*	cDNA, clone: WT002_F22	0
			Gene Bank EST	CJ941014	*Triticumaestivum*	cDNA clone whchan37j15	0
26	Ta-Fg2-P2-F05	198	Gene Bank nr	AK059773	*Oryza sativa*	cDNA clone:006-204-A01	4.00E−48
			Gene Bank EST	EB512735	*Triticumaestivum*	*Fusarium_graminearum*_inculated_wheat_heads, cDNA clone Ta08_04h17	3.00E−82
27	Ta-Fg2-P2-H02	477	Gene Bank nr	CT830060	*Oryza sativa*	Oryza sativa cDNA clone:OSIGCFA236J24	3.00E−149
			Gene Bank EST	EB513252	*Triticumaestivum*	*Fusarium_graminearum*_inculated_wheat_heads, cDNA clone Ta08_06i17	0
28	Ta-Fg2-P2-H04	560	Gene Bank nr	AK330254	*Triticumaestivum*	cDNA, clone: SET4_A05	0
			Gene Bank EST	EB515563	*Triticumaestivum*	*Fusarium_graminearum*_inculated_wheat_heads, cDNA clone Ta10c_03b17	0
29	Ta-Fg2-P2-H05	198	Gene Bank nr	AK335732	*Triticumaestivum*	cDNA clone WT013_K08	2.00E−91
			Gene Bank EST	CN011418	*Triticumaestivum*	Wheat *Fusarium graminearum* infected spike cDNA, cDNA clone WHE3884_A08_A16	4.00E−86
30	Ta-Fg2-P2-H09	425	Gene Bank nr	BT009628	*Triticumaestivum*	cDNA clone wre1n.pk164.e9:fis, similar to methionine sulfoxidereductase.	0
			Gene Bank EST	CJ956666	*Triticumaestivum*	cDNA clone whchul11l08	0
31	Ta-Fg2-P2-D05	186	Gene Bank nr	X62725	*Hordeumvulgare*	Ribosomal protein L17-2	0
			Gene Bank EST	CJ942173	*Triticumaestivum*	cDNA clone whchan40g12	2.00E−89

Two databases were searched with both the BLASTN and BLASTX algorithms: Genbank non-redundant (nr) and EST database. Only sequences related to wheat (*Triticum aestivum*) were placed in the table

Table 2 List of ESTs with accession numbers as deposited in NCBI database of ESTs

No.	dbEST-ID	User-ID	Accession Number	Predicted gene function
1	74222649	Ta-Fg2-P0-80	JK007707	UDP-glucosyltransferase
2	74222650	Ta-Fg2-P0-13	JK007708	Splicing regulator (SRp30a)
3	74222651	Ta-Fg2-P0-331	JK007709	GTPase SAR1 (Sar1.3)
4	74222652	Ta-Fg2-P1-G06	JK007710	Cytokinin-N-glucosyltransferase 1
5	74222653	Ta-Fg2-P1-H12	JK007711	Blue copper protein
6	74222654	Ta-Fg2-P1-A11	JK007712	Histidine-containing phosphotransfer protein 3 (HP)
7	74222655	Ta-Fg2-P1-H04	JK007713	Putative ribosomal protein L35
8	74222656	Ta-Fg2-P1-H06	JK007714	Thaumatin-like protein
9	74222657	Ta-Fg2-P1-G08	JK007715	Thioredoxin M
10	74222658	Ta-Fg2-P1-C11	JK007716	Similar to photosystem I hydrophobic protein
11	74222659	Ta-Fg2-P1-G05	JK007717	Unknown
12	74222660	Ta-Fg2-P2-B01	JK007718	Tryptophan decarboxylase
13	74222661	Ta-Fg2-P2-C04	JK007719	Caffeic acid O-methyltransferase (COMT1) mRNA
14	74222662	Ta-Fg2-P2-C10	JK007720	Phosphatase protein
15	74222663	Ta-Fg2-P2-C11	JK007721	Peroxidase class III
16	74222664	Ta-Fg2-P2-E10	JK007722	Tryptophan synthase beta-subunit (TSB2) mRNA
17	74222665	Ta-Fg2-P2-F04	JK007723	Chitinase 3
18	74222666	Ta-Fg2-P2-H07	JK007724	Putative glucan endo-1,3-beta-D-glucosidase.
19	74222667	Ta-Fg2-P2-H12	JK007725	Receptor kinase (TRKd)
20	74222668	Ta-Fg2-P2-F08	JK007726	Tamdr1 mRNA for multidrug resistance protein
21	74222669	Ta-Fg2-P2-G10	JK007727	Alpha tubulin-4B (TUBA-4B) mRNA
22	74222670	Ta-Fg2-P2-G11	JK007728	Photosystem I subunit N
23	74222671	Ta-Fg2-P2-B06	JK007729	Unknown
24	74222672	Ta-Fg2-P2-D11	JK007730	Unknown
25	74222673	Ta-Fg2-P2-E08	JK007731	Unknown
26	74222674	Ta-Fg2-P2-F05	JK007732	Unknown
27	74222675	Ta-Fg2-P2-H02	JK007733	Unknown
28	74222676	Ta-Fg2-P2-H04	JK007734	Unknown
29	74222677	Ta-Fg2-P2-H05	JK007735	Unknown
30	74222678	Ta-Fg2-P2-H09	JK007736	Unknown
31	74222679	Ta-Fg2-P2-D05	JK007737	Ribosomal protein L17-2

The predicted gene function is based on sequence homology to the best BLAST match, using NCBI databases (http://www.ncbi.nlm.nih.gov/)

to putative glucan endo-1,3-beta-D-glucosidase, and Ta-Fg2-P2-C11 that displayed 99 % homology to peroxidase class III gene, and three clones that matched well with the genes in NCBI: Ta-Fg2-P1-H12 clone to blue copper protein, Ta-Fg2-P1-H06 clone to thaumatin-like protein, and Ta-Fg2-P2-F04 clone to chitinase 3. The remaining up-regulated Ta-Fg2-P2-F05 clone displayed similarity only to an unannotated accession from the GenBank Non-redundant (nr) database.

Cloning of the full-length cDNA of UDP-glucosyltransferase and multiple sequence alignment

Table 1 includes a clone homologous to a UGT, Ta-Fg2-P0-80. This significantly up-regulated clone, which contains a 723-bp insert, showed 99 % similarity to UGT gene (gi: GU248274 in NCBI) and 99 % identity to ESTs induced after powdery mildew infection (gi: CJ942671 in NCBI). A full-length cDNA of the Ta-Fg2-P0-80 clone (TaUGT5) was identified by screening the Sumai 3 cDNA library induced by *F. graminearum* (Al-Taweel et al. 2011) using primers designed according to GU248274 (Online Resource 7). After identification, cloning, and sequencing, the gene was deposited into GenBank under the Accession No. HM133634. The TaUGT5 gene was 1437 bp long and contained an ORF encoding a polypeptide of 478 amino acids with a theoretical molecular weight (MW) of 51.88 kDa and a pI of 6.3. BLAST searches using the deduced amino acid sequences, and the phylogenetic analysis (Online Resource 8, 9) of UGTs indicated that TaUGT5

Table 3 Primers used for real-time RT-PCR

No.	ESTs clone ID	Predicted gene function	Orientation	Sequence (5′ to 3′)
1	Ta-Fg2-P0-80	UDP-glucosyltransferase	F	TAGGGCCGCAACTGCAATC
			R	AAGTTGGTCCAGCTGAGCATG
2	Ta-Fg2-P1-H06	Thaumatin-like protein	F	ACGACATCTCGGTGATCG
			R	TTATTATTGCCACTGCAGGC
3	Ta-Fg2-P2-H07	Putative glucan endo-1,3-beta-D-glucosidase	F	CAGCTCTACAGGTCCAAGGG
			R	CGATGTACTTGATGTTCACGG
4	Ta-Fg2-P2-F04	Chitinase III	F	CCATTATCTCGCAGTCGCT
			R	CTTCTTGACGTCGGTGCTAC
5	Ta-Fg2-P1-H12	Blue copper protein	F	GAAGATCACCCTCCTTGCC
			R	TCTCATCACCCACGTTGAAC
6	Ta-Fg2-P2-C11	Peroxidase III	F	GACTCCGTTGTCGCTCTTG
			R	CGTGTTAAGGTTCTTCTTGAGG
7	Ta-Fg2-P2-F05	Unknown	F	AAAGGCCAGCGTGTACTACC
			R	CTTCTCCATGTCGTCGTGAC
8	UBQ	Ubiquitin	F	AAGACCCTCACCGGCAAGA
			R	GGATACCGGAGACACCGAGA

Optimal oligonucleotide sequences for real-time RT-PCR were predicted using the Primer Express program to prevent faint PCR products as primer dimer and false amplicon

was similar to other plant UGTs at different levels, such as the UGT of *Oryza sativa* (52 % similarity), UGT of *Hordeum vulgare* (51 % similarity), and UGT of *Zea mays* (53 % similarity). TaUGT5 contained a hypothetical acceptor substrate binding region in its N terminus (Poppenberger et al. 2003) and an approximately 40 amino acid UGT consensus sequence also called PSPG (plant secondary product glucosyltransferase signature) box (Li et al. 2001; Hughes and Hughes 1994) in its C terminus.

Real-time quantitative PCR analysis of defense-related genes

In order to evaluate the differential expression of the selected clones in Fg2-infected samples, the transcript accumulations of subtracted genes were analyzed by qPCR for Sumai 3 samples that were infected by two different chemotype isolates, Fg2 (3ADON) and Fg35 (15ADON), at 6, 12, 24, 36, 48, 72, and 144 hai. Sensitive real-time RT-PCR with gene-specific primers (Table 3) was used to quantify transcript levels of the seven selected genes. Figure 5 shows fold changes of differentially expressed genes. The *Y* axis values indicate the relative expression of differentially expressed genes for 3ADON- and 15ADON-infected 'Sumai 3' wheat compared to their expression in the water-inoculated control samples at each sampling time (*X* axis) after inoculation.

The gene expression for clones Ta-Fg2-P0-80 and Ta-Fg2-P1-H06 that showed high similarity to UDP-glucosyltransferase and thaumatin-like protein, respectively, was induced as early as 36 hai with maximum induction occurring at 72 hai for the 3ADON- and 15ADON-infected lines and then decreased sharply by 144 hai. The Ta-Fg2-P2-H07 clone, a putative glucan endo-1,3-beta-D-glucosidase, was induced earlier at 6 hai in response to the pathogen in the plants infected with both chemotypes. The pathogen induced glucosidase transcript accumulation and then quickly reached a higher peak at 72 hai for both chemotypes. However, there was significantly less transcript accumulation in 3ADON-inoculated tissue compared to 15ADON-inoculated tissue. Putative Blue copper protein (Ta-Fg2-P1-H12) transcript accumulation increased dramatically at 48 hai, peaking at 72 hai, followed by a decline in both 3ADON and 15ADON-infected plants by 144 hai. The previous pattern was similar to the transcript

Fig. 5 Fold changes of the expressed genes. Fold changes in transcript levels of differentially expressed genes; **a** UDP-glucosyltransferase, **b** Thaumatin-like protein, **c** Glucosidase, **d** Chitinase III, **e** Blue copper protein, **f** Peroxidase III, **g** Ta-Fg2-P2-F05, between FHB- and water-infected Sumai 3 cultivar at different hours after inoculation (hai) with two different chemotypes of *Fusarium graminearum*. The relative quantity of target gene transcripts was calculated using the comparative cycle threshold (C_t) method. Ubiquitin was used as an endogenous control to normalize the data for input RNA differences between the various samples. 3ADON: Sumai 3 inoculated with Fg2; 15ADON: Sumai 3 inoculated with Fg35; values are mean ± SE of three independent experiments and are normalized to the expression levels of the controls at the same sampling times (set at 0); * indicates values that are statistically significantly different ($P \leq 0.05$) between the two inoculated samples (3ADON/15ADON)

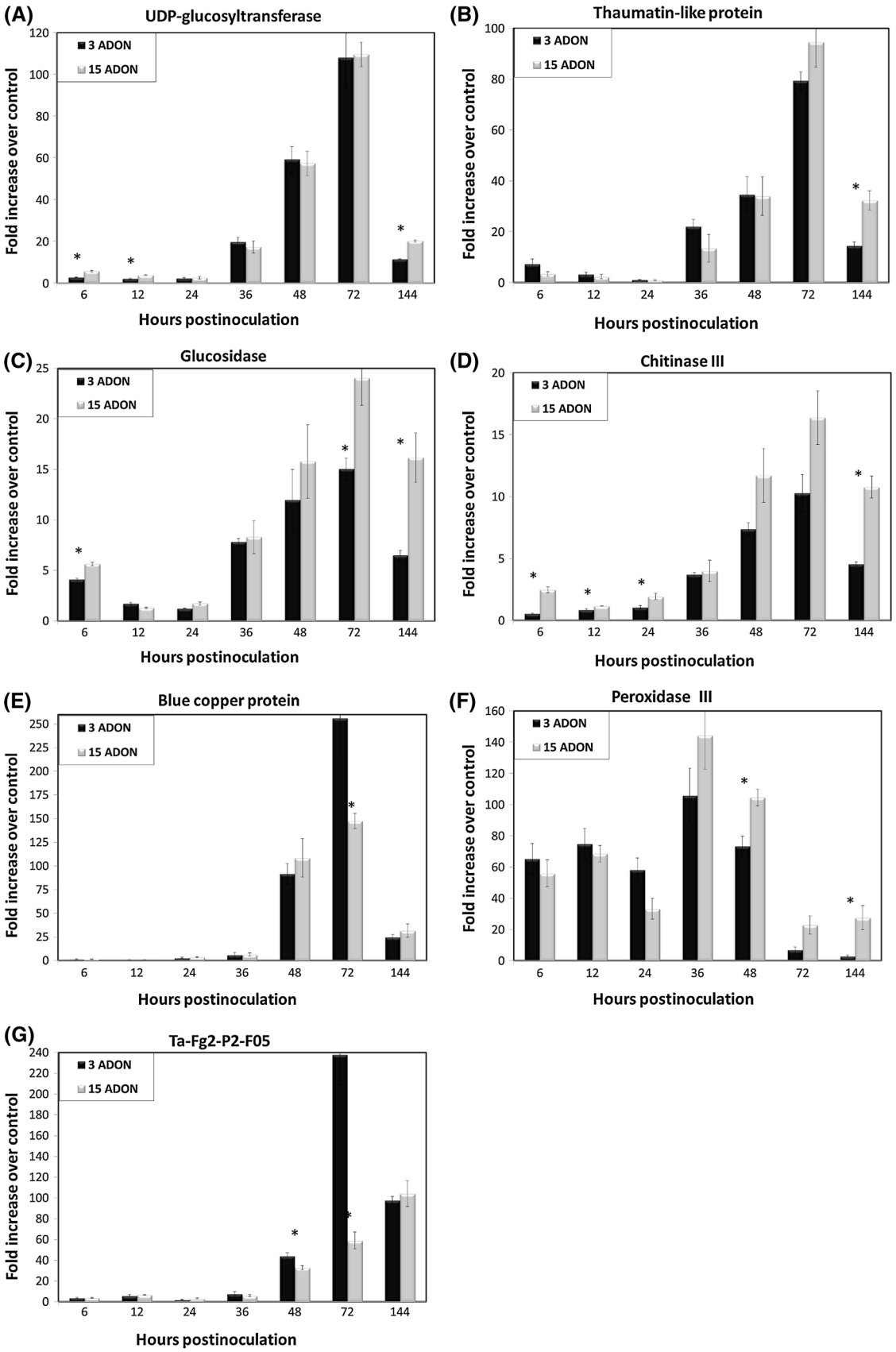
(A)
UDP-glucosyltransferase
3 ADON
15 ADON
Fold increase over control
Hours postinoculation
(B)
Thaumatin-like protein
(C)
Glucosidase
(D)
Chitinase III
(E)
Blue copper protein
(F)
Peroxidase III
(G)
Ta-Fg2-P2-F05

accumulation of the Ta-Fg2-P2-F05 clone (unknown genes). Peroxidase class III gene (Ta-Fg2-P2-C11) was induced right after infection (6 hai) with maximum induction for both lines at 36 hai which then decreased quickly at 72 and 144 hai. The Ta-Fg2-P2-F04 clone, chitinase 3, transcript expression increased at 36 hai, peaking at 72 hai.

Figure 5a shows that there are significant differences at 6, 12, and 144 hai in UDP-glucosyltransferase transcripts for the cultivar Sumai 3 that was infected by the two different FHB-chemotype isolates Fg2 and Fg35 which produce 3ADON and 15ADON, respectively. This difference was clear in putative glucan endo-1,3-beta-D-glucosidase transcripts at 6, 72, and 144 hai (Fig. 5c). The significant difference was only at 144 hai in the case of thaumatin-like protein (Fig. 5b). The expression level of blue copper protein (Fig. 5e) and the unknown gene (Ta-Fg2-P2-F05) (Fig. 5g) for 3ADON-infected spikes was significantly higher than that in 15ADON-infected spikes at 48 and 72 hai, respectively. As for peroxidase III (Fig. 5f), transcript accumulation was significantly higher in 15ADON- compared to 3ADON-infected spikes at 48 and 144 hai. The expression levels of chitinase III enzyme (Fig. 5d) for 15ADON-infected cDNA were higher at all sampling times and significantly higher than that in 3ADON-infected cDNA at 6, 12, 24, and 144 hai.

Discussion

The use of SSH and RT-PCR enabled the identification of 31 clones, one being isolated and characterized. In addition, transcriptome profiling of seven up-regulated putative defense-related genes was undertaken. These genes may be involved in the wheat-pathogen interaction revealing transcript accumulation differences between the non-diseased, 3ADON, and 15ADON infected plants. Additionally, significant differences in gene expression were observed between 3ADON- and 15ADON-infected plants underscoring the significance of a particular chemotype in FHB disease. SSH was the technique of choice for library construction because it can achieve more than 1000-fold enrichment for low abundance differentially expressed cDNAs (Diatchenko et al. 1996), thereby enabling the isolation of rare transcripts that may not be easily obtained from a regular cDNA library. In this study, subsets of clones (1,000) were derived from FHB-SSH library, which made it feasible for us to focus on a small number of genes that responded to the pathogenic stress. Previous studies indicated that Fusarium macroconidia usually germinate later than 6 hai, enter the floret tissue by 36 hai, and spread to nearby uninoculated spikelets after 48 hai (Pritsch et al. 2000). Therefore, in this study, the SSH library was constructed with samples collected at 6, 12, 24, 36, 48, 72, and 144 hai covering the essential period of early fungal infection from spore germination to spread of infection to healthy spikelets.

In this study, based on the chromosome survey sequences generated by the international wheat genome sequencing consortium (IWGSC), UGT is located on chromosomes 7BS (where S represents short arm); glucosidase is present in 3B; chitinase III is located on chromosomes arms 3B and 2DL (where L represents long arm); blue copper-binding protein is located on chromosomes arm 4BL; peroxidase is present in 2DS and 2BS; and thaumatin-like protein is located on chromosome arm 7DL. This study showed that the locations of the identified genes correspond to many of the stable QTL previously identified. To date, Sumai3-derived resistance QTL on 3BS (*Fhb1*) is the most extensively QTL used by breeding programs due to its stable major effect on type II and type III resistance across different genetic backgrounds (Anderson et al. 2001).

A total of 200 non-redundant ESTs were identified, 75 of these sequences showed significant matches to plant genes, and another 51 with significant matches to fungal sequences. Of the seven up-regulated clones, the Ta-Fg2-P0-80 clone (Table 3) showed high homology with UDP-glucosyltransferase (UGT) (99 % with GenBank nr and EST databases). This was an important finding as it has been reported that UGT is able to detoxify deoxynivalenol. Moreover, this enzyme was also found to detoxify the acetylated derivative 15-acetyl-deoxynivalenol (Poppenberger et al. 2003). Glucosylation of trichothecenes represents a detoxification process by plants. Yet in the digestive tract of humans and animals, the mycotoxin-glucoconjugates could easily be hydrolyzed, regenerating the toxin (Poppenberger et al. 2003). Poppenberger et al. (2003) reported that DON-glucosyltransferase 1 (DOGT1) not only detoxified 3ADON but also 15ADON, and expression of the DOGT1 was developmentally regulated and induced by DON as well as salicylic acid, ethylene, and jasmonic acid. Steiner et al. (2009) stated that due to fungal infection, the expression of UDP-glucosyltransferase was drastically elevated suggesting that it has a role in DON detoxification and pathogenesis-related (PR) family protein activation. This might explain our results showing that the expression of UDP-glucosyltransferase was induced in both chemotypes 3ADON and 15ADON and peaked at 72 hai (Fig. 5a).

The clone Ta-Fg2-P1-H06 (Table 3) showed similarity to thaumatin-like protein (TLP). Plants produce a cascade of defense proteins to protect themselves against any pathogen attack, including as many as 17 families of pathogenesis-related (PR) proteins (van Loon et al. 2006). Among them, plant TLPs belong to the PR5 family which shares a high homology with thaumatin (Velazhahan et al. 1999). The plant TLP family showed remarkable in vitro-activity by suppressing hyphal growth or spore germination of various pathogenic fungi presumably through a membrane

permeabilizing mechanism (Abad et al. 1996; Mahdavi et al. 2012). Another role of TLP is the degradation of fungal cell walls by their β-1,3-glucan binding and endo-β-1,3-glucanase activity since β-b-1,3-glucan is a universal component in fungal cell walls (Zareie et al. 2002).

Sumai 3 is known to possess type II resistance that reduces the spread of the fungus in infected tissues (Bai and Shaner 1994, Jayatilake et al. 2011). In this study, Fig. 5b shows that the expression of TLP increased markedly 48 and 72 hai in both 3ADON and 15ADON infected plants, but not at earlier periods of the infection process (e.g., 12 and 24 hai). Previous studies have shown that early recognition of a virulence pathotype of the stripe rust pathogen by wheat leaf cells occurred from 12 hai. In addition, in the resistance interaction, cell death caused by hypersensitive response (HR) was observed as early as 24 hai (Wang et al. 2010). These data indicate that the pathogen-induced accumulation of TLP in the host-pathogen interaction is not a prerequisite to HR, but may be involved in the following defense reactions. The elevated expression of TLP at 48 and 72 hai is in accordance with the results reported by Wang et al. (2010). Two other clones, Ta-Fg2-P2-H07 and Ta-Fg2-P2-F04, (Table 3) displayed high similarities to putative glucan endo-1,3-beta-D-glucosidase (also known as β-1,3-glucanase) and chitinase III, respectively. It has been shown that these enzymes are able to degrade β-1,3-glucans and chitin, the two major structural components of fungal cell walls, and thereby inhibit the growth of the fungus (Arlorio et al. 1992; Nemati and Navabpour 2012). Furthermore, it has been shown that the breakdown products of the fungal cell wall components were released by the activity of two enzymes, act as elicitors of plant defense responses (Collinge et al. 1993; Paré et al. 2005; Thakur and Sohal 2013). It was reported that the expression of glucanase and chitinase was drastically increased in FHB-infected wheat and in fungal hyphae as well, especially at sites where host cells were in close contact with fungal hyphae (Pritsch et al. 2000; Boddu et al. 2006). The accumulation of glucanase and chitinase was much higher after infection of a resistant cultivar compared to a susceptible cultivar, suggesting that this is one possible mechanism for retarding pathogen spread in a resistant cultivar.

The two other clones, which could be categorized under oxidative stress-induced defense genes, are the Ta-Fg2-P1-H12 clone which was homologous to blue copper protein (BCB), and the Ta-Fg2-P2-C11 clone that was homologous to a peroxidase III gene (Table 3). The postulated series of events involved in typical R gene-mediated race-specific resistance include pathogen recognition followed by the triggering of signal transduction cascades that lead to rapid defense mobilization (Hammond-Kosack and Parker 2003). The significant transcripts identified in this study fit into several parts of this system. Firstly, the peroxidase and BCB transcripts are both indicators of an oxidative burst, which is likely to contribute to the HR that is observed in race-specific resistance. During the course of host colonization, toxic stress in the plant occurs from both pathogenic infection and plant production of ROS as a defense response mechanism. In order to protect itself against ROS-induced cellular damage, plants also produce antioxidants, including the PR proteins glutathione-S-transferase (GSTs) and peroxidases (POXs) (Foroud et al. 2012). Peroxidases have been reported to be induced during the resistance response of wheat to the fungal pathogen *F. graminearum* (Mohammadi and Kazemi 2002). In this study, peroxidase transcript levels in both tested samples were observed as early as 6 hai and continued to accumulate until 36 hai. These findings are in agreement with previous results published by Pritsch et al. (2000).

There were two additional clones that were highly expressed under FHB infection (data not shown). The first one was the Ta-Fg2-P1-H04 clone which matched putative ribosomal protein L35 (98 %). It was not surprising to have it expressed at a high level since the proteins of the ribosomes catalyze all of the functions of polypeptide synthesis (Blasi et al. 2002). Ribosomal proteins have also been shown to play roles in stress tolerance and salt adaptation in plants (Wu et al. 2005).

The second clone that had high transcript accumulation was Ta-Fg2-P2-B01 which was identified to code for a tryptophan decarboxylase (TDC). The TDC enzyme converts tryptophan to tryptamine in the catabolism of tryptophan. This enzyme exhibited a high accumulation pattern, indicating that tryptamine or its indole derivatives are specifically increased and may be involved in protecting the plant during infection (Boddu et al. 2006). Biotic and abiotic stresses trigger genes encoding tryptophan biosynthetic and catabolic enzymes (Boddu et al. 2006; Kruger et al. 2002).

Results from this study provided the opportunity to identify biotic and abiotic stress-related genes, and genes which were involved in the basal defense response to *F. graminearum* infection. Of the 31 gene transcripts that were deposited in the NCBI database, gene transcripts encoding DON detoxifying-related gene, PR proteins, and oxidative burst enzymes were quantitatively analyzed. All of these classes of transcripts were found to be qualitatively induced in the wheat infected by two different chemotype isolates of *F. graminearum.*

The qualitative transcript accumulation results showed that the overall transcript number was the greatest at 72 hai. These results were in agreement with the previous studies (Boddu et al. 2006). Although some information about the infection strategies and pathways of *F. graminearum* on wheat is known, the interaction of the pathogen with the host has not yet been fully explored. Boddu et al. (2006)

reported that the fungus can invade through stomatal pores, grow between floral bracts, exhibit subcuticular growth, and penetrate the floral bracts directly. The fungus exhibits subcuticular growth, develops infection hypha, colonizes ovary and floral bract tissue, and sporulates within 72 hai (Pritsch et al. 2000). In addition, other results showed that *F. graminearum* displays traits of a biotroph during the initial 48–72 hai, and then switches to a necrotrophic phase at approximately 72 hai (Kang and Buchenauer 1999), and these findings are compatible with the results of this study.

A key difference between resistant and susceptible plants is the timely recognition of the invading pathogen and the rapid and effective activation of host defense mechanisms. The FHB-resistant line, Sumai 3, used in this study showed that all genes induced under 3ADON chemotype were expressed under 15ADON as well; however, the transcript accumulation levels of the genes responding were almost always higher in the wheat infected by 15ADON isolates (e.g., UDP-glucosyltransferase, thaumatin-like protein, glucosidase, chitinase III, and peroxidase III) especially at the late stages of infection (48–144 hpi). This may lead to the hypothesis that the higher transcript levels of putative defense-related genes under 15ADON may have a role in partially suppressing the virulence of 15ADON chemotype, which may address why isolates from the 3ADON population are more aggressive and seem to produce larger amounts of toxin compared to isolates from the 15ADON population. The significant difference at the transcript expression levels of defense response genes between the two tested chemotypes led us to hypothesize that the pathogen attack (mechanisms) has been slightly altered, and in turn, the plant defense response is modified accordingly. Therefore, further studies on transcriptome profiling will greatly enhance our understanding at the gene expression level of the interaction of different pathogen chemotypes with host plant genes. This information might provide a blueprint for the cellular networks of the pathogen-host interactions and could have an impact on development of FHB-resistant wheat cultivars and disease management.

Conclusion

In this study, an overview of the behavior of wheat transcriptomes to the *F. graminearum* fungus using two different chemotypes was obtained. The transcriptome profiles of seven up-regulated putative defense-related genes were analyzed. One of the key genes encoding UDP-glucosyltransferase, which putatively detoxifies deoxynivalenol, was isolated, cloned, and characterized. Moreover, wheat plant responses to different chemotypes of Fusarium isolates were found to be qualitatively similar but quantitatively different in some sampling times after inoculation. It is postulated that changes in agricultural practices such as use of host resistance and fungicides may drive the pathogen populations to shift to those with greater aggressiveness and DON production. In turn, the host response to pathogen attack changes accordingly. The information obtained in this study could have an impact on development of FHB-resistant wheat cultivars as well as disease management.

Acknowledgments We thank Dr. Guo Xiaowei for doing all the growth cabinet work of wheat spike inoculations with Fusarium spores and the time sensitive harvest of samples. We appreciate professors Muhammad Tahir and Brian Fristensky for their scientific input into the analysis of data. We also thank Dr. Belay Ayele, Paula Parks, Dr. Teresa de Kievit and Dr. Brian Fristensky for critically reading the manuscript. We acknowledge Natural Sciences and Engineering Research Council of Canada (NSERC), Western Grains Research Foundation (WGRF), Agri-Food Research and Development Initiative (ARDI), and the Wheat Breeding Research Cluster (05152) of the Canadian Agri-Science Clusters Initiative for the financial support.

Conflict of interest The authors declare that there is no conflict of interest.

References

Abad LR, D'Urzo MP, Liu D, Narasimhan ML, Reuveni M, Zhu JK, Niu XM, Singh NK, Hasegawa PM, Bressan RA (1996) Antifungal activity of tobacco osmotin has specificity and involves plasma membrane permeabilization. Plant Sci 118:11–23

Alexander NJ, McCormick SP, Waalwijk C, Lee TVD, Proctor RH (2011) The genetic basis for 3-ADON and 15-ADON trichothecene chemotypes in Fusarium. Fung Gen Biol 48:485–495

Al-Taweel K, Fernando WGD, Brule-Babel AL (2011) Construction and characterization of a cDNA library from wheat Infected with *Fusarium graminearum* Fg 2. Int J Mol Sci 12:613–626

Anderson JA, Stack RW, Liu S, Waldron BL, Fjeld AD (2001) DNA markers for Fusarium head blight resistance QTL in two wheat populations. Theor Appl Genet 102:1164–1168

Ansari KI, Doyle SM, Kacprzyk J, Khan MR, Walter S et al (2014) Light influences how the fungal toxin deoxynivalenol affects plant cell death and defense responses. Toxins 6:679–692

Arlorio M, Ludwig A, Boller T, Bonfante P (1992) Inhibition of fungal growth by plant chitinases and beta-1,3-glucanases—a morphological-study. Protoplasma 171:34–43

Bai GH, Shaner G (1994) Scab of wheat—prospects for control. Plant Dis 78:760–766

Blasi F, Ciarrocchi A, Luddi A, Strazza M, Riccio M, Santi S, Arcone R, Pietropaolo C, D'Angelo R, Costantino-Ceccarini E, Melli M (2002) Stage-specific gene expression in early differentiating oligodendrocytes. Glia 39:114–123

Boddu J, Cho S, Kruger WM, Muehlbauer GJ (2006) Transcriptome analysis of the barley-*Fusarium graminearum* interaction. Mol Plant–Microbe Interact 19:407–417

Buerstmayr H, Lemmens M, Ruckenbauer P (1997) Chromosomal location of Fusarium head blight resistance genes in wheat cereal. Res Commun 25:727–728

Buerstmayr H, Lemmens M, Fedak G, Ruckenbauer P, Gill CBS (1999) Back-cross reciprocal monosomic analysis of Fusarium head blight resistance in wheat (*Triticum aestivum* L.). Theor Appl Genet 98:76–85

Buerstmayr H, Ban T, Anderson JA (2009) QTL mapping and marker-assisted selection for Fusarium head blight resistance in wheat: a review. Plant Breed 128:1–26

Collinge DB, Kragh KM, Mikkelsen JD, Nielsen KK, Rasmussen U, Vad K (1993) Plant chitinases. Plant J 3:31–40

Cuthbert PA, Somers DJ, Thomas J, Cloutier S, Brule- Babel A (2006) Fine mapping *Fhb1*, a major gene controlling Fusarium head blight resistance in bread wheat (*Triticum aestivum* L.). Theor Appl Genet 112:1465–1472

Diatchenko L, Laut YC, Campbellt AP, Chenchik A, Moqadam F, Huang B, Lukyanovt S, Lukyanovt K, Gurskayat N, Sverdlovt ED, Siebert PD (1996) Suppression subtractive hybridization: a method for generating differentially regulated or tissue-specific cDNA probes and libraries. Proc Natl Acad Sci USA 93:6025–6030

Foroud NA, Ouellet T, Laroche A, Oosterveen B, Jordan MC, Ellis BE, Eudes F (2012) Differential transcriptome analyses of three wheat genotypes reveal different host response pathways associated with Fusarium head blight and trichothecene resistance. Plant Pathol 61:296–314

Goswami RS, Kistler HC (2004) Heading for a disaster: *Fusarium graminearum* on cereal crops. Mol Plant Pathol 5:515–525

Guo XW, Brock-Seow MS, Fernando WGD (2008) Population structure, chemotype diversity, and potential chemotype shifting of *Fusarium graminearum* in wheat fields of Manitoba. Plant Dis 92:756–762

Hallen-Adams HE, Wenner N, Kuldau GA, Trail F (2011) Deoxynivalenol biosynthesis-related gene expression during wheat kernel colonization by *Fusarium graminearum*. Phytopathol 101:1091–1096

Hammond-Kosack KE, Parker JE (2003) Deciphering plant-pathogen communication: fresh perspectives for molecular resistance breeding. Curr Opin Biotechnol 14:177–193

Harris LJ, Gleddie SC (2001) A modified Rpl3 gene from rice confers tolerance of the *Fusarium graminearum* mycotoxin deoxynivalenol to transgenic tobacco. Physiol Mol Plant Pathol 58:173–181

Hughes J, Hughes MA (1994) Multiple secondary plant product UDP-glucose glucosyltransferase genes expressed in cassava (Manihot esculenta Crantz) cotyledons. DNA Seq 5:41–49

Jayatilake DV, Bai GH, Dong YH (2011) A novel quantitative trait locus for Fusarium head blight resistance in chromosome 7A of wheat. Theor Appl Genet 122:1189–1198

Kang Z, Buchenauer H (1999) Immunocytochemical localization of Fusarium toxins in infected wheat spikes by *Fusarium culmorum*. Physiol Mol Plant Pathol 55:275–288

Kang Z, Buchenauer H (2000a) Ultrastructural and cytochemical studies on cellulose, xylan and pectin degradation in wheat spikes infected by *Fusarium culmorum*. J Phytopathol 148:263–275

Kang Z, Buchenauer H (2000b) Ultrastructural and immunocytochemical investigation of pathogen development and host responses in resistant and susceptible wheat spikes infected by *Fusarium culmorum*. Physiol Mol Plant Pathol 57:255–268

Kruger WM, Pritsch C, Chao S, Muehlbauer GJ (2002) Functional and comparative bioinformatic analysis of expressed genes from wheat spikes infected with *Fusarium graminearum*. Mol Plant–Microbe Interact 15:445–455

Li Y, Baldauf S, Lim EK, Bowles DJ (2001) Phylogenetic analysis of the UDP-glycosyltransferase multigene family of *Arabidopsis thaliana*. J Biol Chem 276:4338–4343

Liu S, Hall MD, Griffey CA, McKendry AL (2009) Meta-analysis of QTL associated with Fusarium head blight resistance in wheat. Crop Sci 49:1955–1968

Lucyshyn D, Busch BL, Abolmaali S, Steiner B, Chandler E, Sanjarian F, Mousavi A, Nicholson P, Buerstmayr H, Adam G (2007) Cloning and characterization of the ribosomal protein L3 (*RPL3*) gene family from *Triticum aestivum*. Mol Genet Genomics 277:507–517

Mahdavi F, Sariah M, Maziah M (2012) Expression of rice thaumatin-like protein gene in transgenic banana plants enhances resistance to Fusarium Wilt. Appl Biochem Biotechnol 166:1008–1019

Miller JD, Arnison PG (1986) Degradation of deoxynivalenol by suspension-cultures of the Fusarium head blight resistant wheat cultivar Frontana. Can J Plant Pathol 8:147–150

Mitterbauer R, Adam G (2002) *Saccharomyces cerevisae* and *Arabidopsis thaliana*: useful model systems for the identification of molecular mechanisms involved in resistance of plants to toxins. Eur J Plant Pathol 108:699–703

Mohammadi M, Kazemi H (2002) Changes in peroxidase and polyphenol oxidase activities in susceptible and resistant wheat heads inoculated with *Fusarium graminearum* and induced resistance. Plant Sci 162:491–498

Nemati M, Navabpour S (2012) Study on quantitative expression pattern of oxalate oxidase and β -1,3 glucanase genes under *Fusarium graminearum* treatment in wheat by quantitative Real time PCR. Intl J Agri Crop Sci 4:443–447

Paré PW, Farag MA, Krishnamachari V, Zhang H, Ryu CM, Kloepper JW (2005) Elicitors and priming agents initiate plant defense responses. Photosynth Res 85:149–159

Placinta CM, D'Mello JPF, Macdonald AMC (1999) A review of worldwide contamination of cereal grains and animal feed with Fusarium mycotoxins. Anim Feed Sci Technol 78:21–37

Poppenberger B, Berthiller F, Lucyshyn D, Sieberer T, Schuhmacher R, Krska R, Kuchler K, Glossl J, Luschnig C, Adam G (2003) Detoxification of the Fusarium mycotoxin deoxynivalenol by a UDP-glucosyltransferase from *Arabidopsis thaliana*. J Biol Chem 278:47905–47914

Pritsch C, Muehlbauer GJ, Bushnell WR, Somers DA, Vance CP (2000) Fungal development and induction of defense response genes during early infection of wheat spikes by *Fusarium graminearum*. Mol Plant-Microbe Interact 13:159–169

Puri KD, Zhong S (2010) The 3ADON population of *Fusarium graminearum* found in North Dakota is more aggressive and produces a higher level of DON than the prevalent 15ADON population in spring wheat. Phytopathol 100:1007–1014

Schmidt-Heydt M, Rüfer CE, Abdel-Hadi A, Magan N, Geisen R (2010) The production of aflatoxin B1 or G1 by *Aspergillus parasiticus* at various combinations of temperature and water activity is related to the ratio of *aflS* to *aflR* expression. Mycotoxin Res 26:241–246

Schmittgen TD, Livak KJ (2008) Analyzing real-time PCR data by the comparative Ct method. Nat Protoc 3:1101–1108

Steiner B, Kurz H, Lemmens M, Buerstmayr H (2009) Differential gene expression of related wheat lines with contrasting levels of head blight resistance after *Fusarium graminearum* inoculation. Theor Appl Genet 118:753–764

Sugita-Konishi Y, Kumagai S (2005) Toxicity of mycotoxins related with head blight diseases in wheat and establishment of provisional standard for tolerable level of DON in wheat. Mycotoxins 55:49–53

Thakur M, Sohal BS (2013) Role of elicitors in inducing resistance in plants against pathogen infection. ISRN Biochem. doi:10.1155/2013/762412 Article ID 762412

Van Loon LC, Rep M, Pieterse CMJ (2006) Significance of inducible defense-related proteins in infected plants. Annu Rev Phytopathol 44:135–162

Velazhahan R, Datta S, Muthukrishnan S (1999) The PR-5 family: thaumatin-like proteins in plants pathogenesis related proteins in plants. CRC Press, Boca Raton, pp 107–129

Waalwijk C, Kastelein P, Vries ID, Kerenyi Z, Lee TVD, Hesselink T, Kohl J, Kema G (2003) Major changes in *Fusarium* spp. in wheat in the Netherlands. Eur J Plant Pathol 109:743–754

Wang X, Tang C, Deng L, Cai G, Liu X, Liu B, Han Q, Buchenauer H, Wei G, Han D, Huang L, Kang Z (2010) Characterization of a pathogenesis-related thaumatin-like protein gene *TaPR5* from wheat induced by stripe rust fungus. Physiol Plantarum 139:27–38

Ward TJ, Clear RM, Rooney AP, O'Donnell K, Gaba D, Patrick S, Starkey DE, Gilbert J, Geiser DM, Nowicki TW (2008) An adaptive evolutionary shift in Fusarium head blight pathogen populations is driving the rapid spread of more toxigenic *Fusarium graminearum* in North America. Fungal Genet Biol 45:473–484

Windels CE (2000) Economic and social impacts of Fusarium head blight: changing farms and rural communities in the Northern Great Plains. Phytopathol 90:17–21

Wu YR, Wang QY, Ma YM, Chu CC (2005) Isolation and expression analysis of salt up-regulated ESTs in upland rice using PCR-based subtractive suppression hybridization method. Plant Sci 168:847–853

Xie M, Wang M (1999) Relationship between wheat scab disease severity and DON content. Acta Phytopathol Sin 29:41–44

Xu X, Nicholson P (2009) Community ecology of fungal pathogens causing wheat head blight. Annu Rev Phytopathol 47:83–103

Yu JB, Bai GH, Zhou WC, Dong YH, Kolb FL (2008) Quantitative trait loci for Fusarium head blight resistance in a recombinant inbred population of Wangshuibai/Wheaton. Phytopathol 98:87–94

Zareie R, Melanson DL, Murphy PJ (2002) Isolation of fungal cell wall degrading proteins from barley (*Hordeum vulgare* L.) leaves infected with *Rhynchosporium secalis*. Mol Plant–Microbe Interact 15:1031–1039

Zhang H, Zhang Z, Lee TVD, Chen WQ, Xu J, Xu JS, Yang L, Yu D, Waalwijk C, Feng J (2010) Population genetic analyses of *Fusarium asiaticum* populations from barley suggest a recent shift favoring 3ADON producers in Southern China. Phytopathol 100:328–336